Concentration Dependent Diffusion of Self-Propelled Rods

Arshad Kudrolli

Department of Physics, Clark University, Worcester, Massachusetts 01610, USA

(Received 28 August 2009; published 23 February 2010)

We examine the persistent random motion of self-propelled rods (SPR) as a function of the area fraction ϕ and study the effect of steric interactions on their diffusion properties. SPR of length l and width w are fabricated with a spherocylindrical head attached to a beaded chain tail, and show directed motion on a vibrated substrate. The mean square displacement (MSD) on the substrate grows linearly with time t for $\phi < w/l$, before displaying caging as ϕ is increased, and stops well below the close packing limit. Direction autocorrelations decay progressively slower with ϕ. We describe the observed decrease of SPR propagation speed $c(\phi)$ with a tube model. Further, MSD parallel to the SPR collapse with $\tau = l/c(\phi)$ and scales as $(lt/\tau)^2$, and MSD in the perpendicular direction grows progressively slower than $l^2 t/\tau$ with ϕ, consistent with dynamics inside a thinning tube.

DOI: 10.1103/PhysRevLett.104.088001 PACS numbers: 45.70.Qj, 05.65.+b

Motivated by dynamical self-assembly of complex systems, the collective behavior of bacterial colonies, animal herds, and self-propelled autonomous particles such as catalytic nanorods and vibrated grains is a topic of intense investigation [1–4]. A typical system can contain thousands if not millions of individuals which move and interact with each other. Random walk models are being developed to describe the motion of an individual moving under various conditions [5], and phenomenological and hydrodynamic models have been introduced to capture their collective behavior [6].

Diffusion can be determined not only by the propulsion speed and polarity of the individual but also by steric interactions with neighbors. Using spheres vibrated on a substrate, Reis *et al.* [7] have shown full arrest in a crystalline phase which occurs below close packing, and caging dynamics in an intermediate hexatic phase broadly consistent with colloidal and other thermal hard particle systems. In rods, nematic or tetratic ordering can occur depending on the concentration and aspect ratio in thermal and athermal systems [8–10]. While diffusion of entangled rodlike molecules has been discussed with a tube model [11,12], with the exception of a recent study on rods in fluidized beds at moderate area fraction [13], there are no investigations of the effect of concentration on the diffusion of self-propelled particles. Self-propelled particles are manifestly out-of-equilibrium, and principles developed for equilibrium systems cannot be applied directly to such systems. To establish transport properties of active particles which can simply arise because of self-propulsion and steric interactions, we investigate dynamics of mechanical self-propelled rods (SPR) of length l and width w.

Our SPR are constructed with a hollow steel spherocylindrical shaped head 11.0 mm in length and 4.0 mm wide and beaded chain tail with diameter $d = 3.125$ mm which are connected to each other with a flexible link which can take lengths uniformly between 0 and 1.1 mm [see Fig. 1(a)]. One of the beads is clipped inside the spherocylinder as shown in Fig. 1(a) shifting its center of mass towards the tail. As demonstrated previously, such rods undergo directed motion [4] because of an unbalanced force of friction acting towards the center of mass of the particle at the point of contact [14]. The SPR aspect ratio l/w was varied from 4.5 to 11 by changing the tail from 1 to 5 beads. The flexible links allow the bonds between the beads to be distributed uniformly between $\pm\pi/4$ radians, and the resulting chain persistence length is 10 times the number of links [15], which is greater than in SPR used in our experiments. While this flexibility mimics semirigid nature of many organisms, it also results in added noise which prevents boundary aggregation observed in Ref. [4],

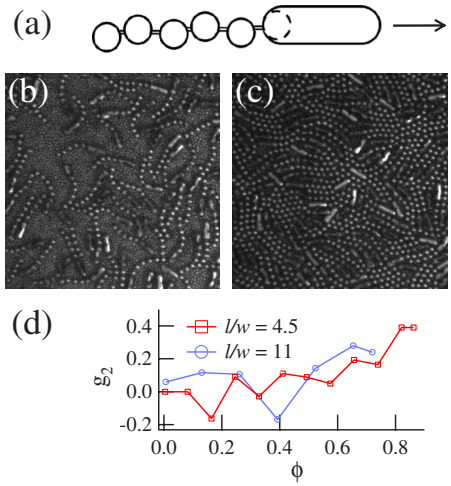

FIG. 1 (color online). (a) Schematic of mechanical self-propelled rods (SPR) of total length l and width w composed of a spherocylindrical head and a flexible beaded chain which moves in the direction of the head on a vibrated substrate. Images of SPR with an aspect ratio $l/w = 11$ for (b) $\phi = 0.32$, and (c) $\phi = 0.72$. No long range order is observed although some short range appears for higher ϕ. (d) To quantify short range order, the angular correlation function $g_2(r)$ plotted as a function of the area fraction ϕ for $l < r < 2l$.

as well prevents the occurrence of highly ordered tetratic phases.

The SPR number is varied to change the SPR concentration or area fraction ϕ which is given by their number times the area occupied by the spherocylindrical head and the beads in the tail of the SPR divided by the area of the container. The container with radius $r_c = 142.5$ mm is vibrated sinusoidally with a frequency $f = 50$ Hz and peak acceleration $a = 3g$, where g is the acceleration of gravity. The resulting vertical motion of the SPR is small compared to the size of the particle and the diffusion dynamics can be considered as two-dimensional because SPR do not leap over each other. A rough substrate is obtained by gluing a layer of 1 mm steel beads which induces fluctuations in the SPR direction. We thus obtain motion with a persistent direction over a length which is much less than r_c.

A Pixelink 1000×1000 pixel camera is mounted above the container. In order to observe diffusion of particles over a wide time scale, we use a tracer technique. Up to 5 chrome plated SPR particles which reflect light from an overhead light source into the camera are tracked among SPR colored black which otherwise have identical properties. The tracer SPR are located by first identifying bright pixels, and then its center and direction is determined by fitting an ellipse to the bright region denoting the particle and identifying the major axis. We find that the SPR position on the substrate in the laboratory reference frame $\mathbf{r}(t)$ at time t can be tracked to within 0.5 mm for an extended period of time with a frame rate of approximately 15.3 Hz. Limited experiments were also performed with a 1000 Hz frame rate camera and it was found that the instantaneous SPR velocity fluctuations about mean decorrelated within $1/f$. In the experiments discussed here, the SPR were tracked from 600 s for the lowest ϕ where motion is rapid and up to 3600 s for the highest ϕ when SPR appear arrested.

Thermal rods are well known to undergo a nematic transition when ϕ is increased above $\frac{3\pi w}{2l}$ in two dimensions for $l/w > 3\pi/2$, because such a state is entropically favorable [8,9]. Therefore, for $l/w = 4.5$, no nematic order is expected and for $l/w = 11$, nematic order may occur above $\phi = 0.428$. Further, the concentrations are expected to shift to higher concentrations for flexible rods [11]. Although SPR are not thermal, images shown in Figs. 1(b) and 1(c) show trends consistent with this behavior, with no significant order noted for $\phi = 0.32$, and some short range nematic order for $\phi = 0.72$. To obtain a quantitative measure of order, we calculated the angular correlation function $g_n(r)$ for two SPR separated by distance r given by $g_n(r) = \langle \cos(n[\theta(\mathbf{r}_0) - \theta(\mathbf{r} + \mathbf{r}_0)]) \rangle$, where, $n = 2$, and 4, is used to detect any nematic and tetratic order respectively, θ is the angle the axis of SPR located at $\mathbf{r}_0$, and $\langle \cdots \rangle$ refers to averaging over pairs of tracer particles and over time. In all cases, $g_n(r)$ fluctuates around zero indicating a lack of angular correlation except for $r \sim l$, where g_2 was observed to increase moderately with ϕ [see Fig. 1(d)].

Typical SPR motion observed over a time interval of 600 s for various ϕ is shown in Fig. 2. For low ϕ, SPR are observed to move freely, but as ϕ is increased, SPR show caging motion for intermediate ϕ, and appear trapped for $\phi = 0.72$, well below the close packed limit of spherocylindrical rods which is between 0.906 and 1 depending on l/w in a large enough container. Superficially, this behavior seems similar to the caging dynamics observed with spheres [7], but in fact the SPR dynamics is fundamentally different. In order to quantify the observed behavior, we calculate the SPR mean square displacement (MSD) on the vibrated substrate using $\langle (\mathbf{r}(t + t_0) - \mathbf{r}(t_0))^2 \rangle$. Where angular brackets denote averaging over initial times t_0, and over 5 tracers. MSD is plotted in Fig. 3(a) over a wide range of ϕ. While MSD grows linearly with t for intermediate time scales for $\phi < w/l$, at progressively higher ϕ, it shows growth ranging from superlinear to sublinear, and arrest. If a particle moves with constant velocity, then MSD is expected to grow as t^2. However, for a noisy driving source as in a rough vibrating plate, MSD can be different from t^2. Further, if the direction persistence time is much less than the time needed to cross the container, then MSD can be expected to cross over to grow as t [16]. Finally, the MSD can be expected to asymptote to $\frac{1}{2} r_c^2 \sim 120$ cm^2 assuming that the SPR reflects off the boundary and uniformly covers the entire container.

To unravel these complex interactions, we separate the 3 degrees of freedom allowed to a rod in two dimensions, and examine its rotation and translation in parallel and perpendicular direction to its axis, guided by the tube picture of diffusion for rods [12]. To measure the direction persistence time scale of SPR, we evaluate the direction autocorrelation function $C_D(t) = \langle \mathbf{\Theta}(t_0) \cdot \mathbf{\Theta}(t + t_0) \rangle$ [see Fig. 3(b)], where, $\mathbf{\Theta}(t)$ is the angular orientation vector

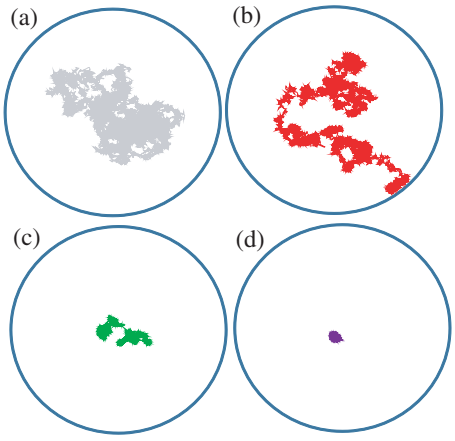

FIG. 2 (color online). Typical trajectories of a SPR with $l/w = 11$ over a 600 s time interval for $\phi = 0.13$ (a), 0.32 (b), 0.58 (c), and 0.72 (d). SPR diffuse freely at low ϕ, shows caging and cage-breaking for $\phi = 0.32$, 0.58, and appears arrested for $\phi = 0.72$.

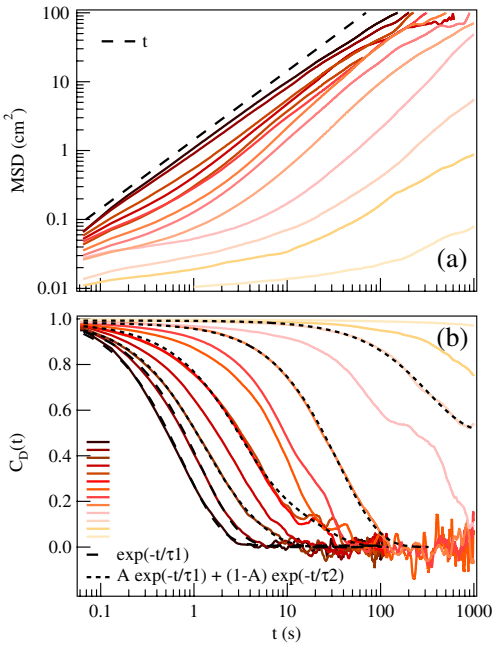

FIG. 3 (color online). (a) Mean square displacement (MSD) of SPR ($l = 15.0$ mm and $l/w = 4.5$) for $0.004 \leq \phi \leq 0.862$. (b) Corresponding SPR direction autocorrelation function $C_D(t)$ decays progressively slowly with ϕ. τ_1 and τ_2 are time constants and A is the relative strength obtained by fitting $C_D(t)$.

of the SPR in the laboratory frame of reference at time t, the angular brackets denote averaging over the 5 tracer particles, and over initial time t_0. For uncorrelated changes in the direction of SPR, $C_D(t) = \exp(-t/\tau_p)$, where τ_p is a measure of the direction persistence time scale. Indeed, $C_D(t)$ can be described by an exponential function for $\phi < w/l$, but at higher ϕ, it appears to be better described by the sum of two exponential functions with a fast and a slow decay, as was also noted in Ref. [13]. Examples of fits are shown in Fig. 3(b). Regardless of the fitting function, $C_D(t)$ shows that the rotational motion gets progressively suppressed as ϕ increases, hand-in-hand with the decreases in MSD.

Next, we examine the SPR displacements in a body frame of reference which is located on the tracer particle with x, y axes oriented parallel and perpendicular to SPR, respectively. Then the corresponding MSD are given by $\langle \Delta x^2(t) \rangle = \langle (x(t_0) - x(t_0 + t))^2 \rangle$ and $\langle \Delta y^2(t) \rangle = \langle (y(t_0) - y(t_0 + t))^2 \rangle$, where $\langle \cdots \rangle$ denotes averaging over initial time t_0 and tracer particles. Introducing a time scale taken by the SPR to move its length

$$\tau = l/c(\phi), \tag{1}$$

we plot the MSD in the parallel and perpendicular directions versus time scaled with τ in Fig. 4. The range of ϕ plotted is where SPR has moved at least l and $c(\phi) > 0$. From Figs. 4(a) and 4(b), we note the scaled MSD all go as $(t/\tau)^2$ for long time t, i.e., $\langle \Delta x^2(t) \rangle \to (c(\phi)t)^2$. Further, the crossover to this scaling is similar for all cases. On the

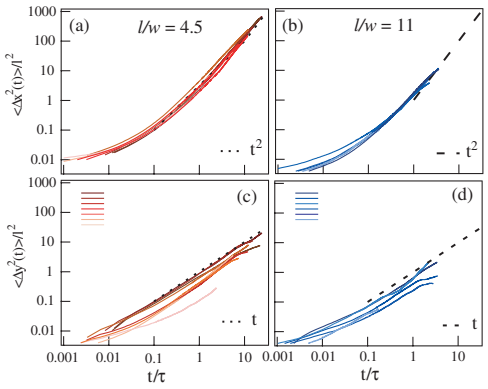

FIG. 4 (color online). Body frame MSD in (a),(b) parallel direction and (c),(d) perpendicular direction as a function of time scaled with the time to travel a SPR length τ. (a), (c) $l/w = 11$ for $0.0041 \leq \phi \leq 0.739$, and (b),(d) $l/w = 4.5$ for $0.0064 \leq \phi \leq 0.643$.

other hand, MSD in the perpendicular direction shown in Figs. 4(c) and 4(d) scales as t/τ.

If a SPR performs a directed random walk along its axis, and fluctuates randomly perpendicularly to axis, then $\langle \Delta x^2(t) \rangle \to (c(\phi)t)^2$ and $\langle \Delta y^2(t) \rangle \to 2D_{\text{per}}(\phi)t$, where $c(\phi)$ and $D_{\text{per}}(\phi)$ are the ϕ dependent SPR mean speed and diffusion constant perpendicular to SPR direction, respectively. Thus by fitting the MSDs in the long time limit, we measure and plot $c(\phi)$ normalized by the speed for a single SPR $c(\phi_0) = 3.2$ mm s^{-1} and 1.02 mm s^{-1} for $l/w = 4.5$ and 11 in Fig. 5(a), and $D_{\text{per}}(\phi)$ in Fig. 5(b), respectively. Both scaled quantities show systematic decrease with ϕ, and go to 0 before SPR are jammed as noted as well in the discussion of Fig. 2. The speed for a SPR with longer tail can be expected to be lower because the propulsion force F_p due to the spherocylindrical head is same but drag increases with its length. Assuming that the drag force is proportional to the number of elements in the SPR, we have for a n-bead SPR: $F_p - (n + 1)F_d = 0$, where the drag force per unit element $F_d \sim c_n \xi$, with ξ a friction coefficient according to the Rouse model [15]. The ratio of speeds for n and m beads is then $c_n/c_m = (m + 1)/(n + 1)$. Therefore, the speeds for a SPR with 5 bead tail can be expected to be lower by a factor of 3, which is indeed the case.

To explain the observed ϕ dependence, we use a modified tube model of rodlike molecules [11,12], where it was argued that entangled rods diffuse more easily along its axis. There, a self-consistency argument was used to calculate the effect of density on diffusion provided the rods were still randomly ordered. Let us consider a SPR which moves as shown in Fig. 5. Unlike rod molecules considered in Ref. [12] which diffuse and change neighbors given by the diffusion time scale, we postulate that this time scale in our SPR case is set by the time τ. Therefore, the total time $t_t = 1/c(\phi)$ taken by a SPR to travel a unit distance can be broken in two components, $t_t = t_m + n_c t_w$, where t_m is the time it would take the SPR to move the distance unhin-

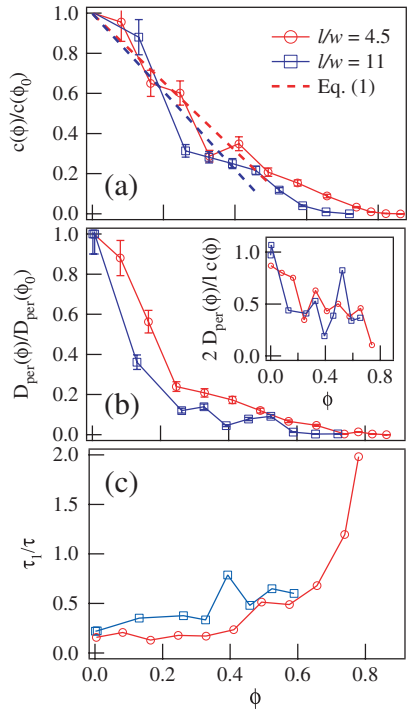

FIG. 5 (color online). (a) SPR mean speed as a function of ϕ, normalized by corresponding speed of single SPR. Equation (2) with $\alpha = 1.6 \pm 0.1$ is observed to describe the decrease in speed in a regime where g_2 shows little local order. (b) The diffusion constant perpendicular to the SPR direction decays with ϕ. Inset: The decrease is faster in the perpendicular direction compared with in the parallel direction consistent with a tube picture.

dered by other particles and therefore $t_m = 1/c(\phi_0)$, t_w is the time a SPR is stuck in place because of an obstructing SPR, n_c is the number of obstructing SPR encountered during the translation. Assuming uncorrelated collisions, $n_c \sim \sqrt{2}c(\phi_0)\phi/lt_m$, where $\sqrt{2}$ arises because of relative velocity of SPR. Now, because all SPR are identical and move with the same speed, the average time for an obstructing SPR to move out of the path can be argued to be $t_w \sim (l/2 + w)/c(\phi)$, assuming isotropic angle distributions when SPR meet. Substituting n_c and t_w above, and solving for $c(\phi)$, we obtain

$$c(\phi) = c(\phi_0)[1 - \alpha(1/\sqrt{2} + \sqrt{2}w/l)\phi]. \qquad (2)$$

Where α is a constant which should be of order 1. The observed $c(\phi)$ in Fig. 5 is described by Eq. (2) with $\alpha = 1.6 \pm 0.1$ for $\phi < 0.5$, where g_2 shows no local order. Above, $\phi > 0.5$, it is possible that $c(\phi)$ approaches zero less slowly because flexibility and alignment of SPR may allow it to move more easily and therefore faster than implied by isotropic entanglement. Further, $c(\phi) \to 0$ somewhat at a lower ϕ for greater l/w possibly due to greater entanglement which is not captured by this simplified model.

In the tube picture, the rod diffuses a distance of order l before it can change neighbors, and for semidilute concentration, it can change directions by order tube radius once it has moved this distance. As ϕ is increased the tube radius decreases, and therefore fluctuations in the transverse and rotational modes are expected to decrease because of increased collisions with neighbors. From the t/τ dependence of $\langle \Delta y^2(t) \rangle$, we have $D_{\rm per}(\phi) \lesssim \frac{1}{2} lc(\phi)$. The ratio $\frac{2D_{\rm per}(\phi)}{lc(\phi)}$ is plotted in the inset to Fig. 5(b) and shows that transverse fluctuations are indeed suppressed relative to the longitudinal or parallel direction. Further, in Fig. 5(c), we plot the dominant time scale τ_1 in the decay of $C_D(t)$ obtained from the exponential fits shown in Fig. 3(b) normalized by τ. τ_1 is observed to increase relative to τ with ϕ also showing that changes of direction are suppressed relative to translation.

Therefore these measures of translation and rotation motion of the SPR are consistent with the picture that they move along a tube which gets narrower as ϕ increases, and their advance along the tube is blocked increasingly with ϕ because other SPR act as barriers. Finally, SPR progress is arrested well below the close packing concentration which depends on l/w.

The work was supported by the National Science Foundation under Grant No. DMR-0605664. We thank Jessica Baker for help in assembling the particles, and Michael Berhanu for comments.

[1] A. Sokolov, I. S. Aranson, J. O. Kessler, and R. E. Goldstein, Phys. Rev. Lett. **98**, 158102 (2007).
[2] I. D. Couzin, J. Krause, N. R. Franks, and S. A. Levin, Nature (London) **433**, 513 (2005).
[3] P. Dhar *et al.*, Nano Lett. **6**, 66 (2006).
[4] A. Kudrolli, G. Lumay, D. Volfson, and L. Tsimring, Phys. Rev. Lett. **100**, 058001 (2008).
[5] E. A. Codling, M. J. Plank, and S. Benhamou, J. R. Soc. Interface **5**, 813 (2008).
[6] T. Vicsek *et al.*, Phys. Rev. Lett. **75**, 1226 (1995); J. Toner, Y. Tu, and S. Ramaswamy, Ann. Phys. (Berlin) **318**, 170 (2005); F. Peruani, A. Deutsch, and M. Bär, Phys. Rev. E **74**, 030904(R) (2006); A. Baskaran and M. C. Marchetti, Phys. Rev. Lett. **101**, 268101 (2008).
[7] P. M. Reis, R. A. Ingale, and M. D. Shattuck, Phys. Rev. Lett. **98**, 188301 (2007).
[8] L. Onsager, Ann. N.Y. Acad. Sci. **51**, 627 (1949).
[9] J. Galanis *et al.*, Phys. Rev. Lett. **96**, 028002 (2006).
[10] V. Narayan, N. Menon, and S. Ramaswamy, J. Stat. Mech. (2006) P01005.
[11] M. Doi and S. F. Edwards, *The Theory of Polymer Dynamics* (Clarendon Press, Oxford, 1999).
[12] S. F. Edwards and K. E. Evans, J. Chem. Soc., Faraday Trans. 2 **78**, 113 (1982).
[13] L. J. Daniels, Y. Park, T. C. Lubensky, and D. J. Durian, Phys. Rev. E **79**, 041301 (2009).
[14] D. Volfson, A. Kudrolli, and L. Tsimring, Phys. Rev. E **70**, 051312 (2004).
[15] K. Safford, Y. Kantor, M. Kardar, and A. Kudrolli, Phys. Rev. E **79**, 061304 (2009).
[16] P. M. Kareiva and N. Shigesada, Oecologia **56**, 234 (1983).